

1 **The amplitude of fNIRS hemodynamic response in the visual cortex unmasks**
2 **autistic traits in typically developing children**

3

4 Raffaele Mazziotti^{1,2‡}, Elena Scaffei^{2,3‡}, Eugenia Conti³, Viviana Marchi³, Riccardo Rizzi^{2,3},
5 Giovanni Cioni^{3,4}, Roberta Battini^{3,4}, Laura Baroncelli^{1,3*}

6

7 [1] Institute of Neuroscience, National Research Council (CNR), I-56124, Pisa, Italy

8 [2] Department of Neuroscience, Psychology, Drug Research and Child Health NEUROFARBA, University of
9 Florence, I-50135, Florence, Italy

10 [3] Department of Developmental Neuroscience, IRCCS Stella Maris Foundation, I-56128, Pisa, Italy

11 [4] Department of Clinical and Experimental Medicine, University of Pisa, Pisa, Italy

12

13 *To whom correspondence should be addressed: baroncelli@in.cnr.it

14 ‡These authors equally contributed to the work

15

16

17

18

19

20

21

22

23

24

25

26

27

28

29

30

31

32

33

34

35

36

37

38

39 **Abstract**

40 **Autistic traits represent a continuum dimension across the population, with**
41 **autism spectrum disorder (ASD) being the extreme end of the distribution.**
42 **Accumulating evidence shows that neuroanatomical and neurofunctional**
43 **profiles described in relatives of ASD individuals reflect an intermediate**
44 **neurobiological pattern between the clinical population and healthy controls.**
45 **This suggests that quantitative measures detecting autistic traits in the**
46 **general population represent potential candidates for the development of**
47 **biomarkers identifying early pathophysiological processes associated with**
48 **ASD. Functional near-infrared spectroscopy (fNIRS) has been extensively**
49 **employed to investigate neural development and function. In contrast, the**
50 **potential of fNIRS to define reliable biomarkers of brain activity has been**
51 **barely explored. Features of non-invasiveness, portability, ease of**
52 **administration and low-operating costs make fNIRS a suitable instrument to**
53 **assess brain function for differential diagnosis, follow-up, analysis of**
54 **treatment outcomes and personalized medicine in several neurological**
55 **conditions. Here, we introduce a novel standardized procedure with high**
56 **entertaining value to measure hemodynamic responses (HDR) in the occipital**
57 **cortex of adult subjects and children. We found that the variability of evoked**
58 **HDR correlates with the autistic traits of children, assessed by the Autism-**
59 **Spectrum Quotient. Interestingly, HDR amplitude was especially linked to**
60 **social and communication features, representing the core symptoms of ASD.**
61 **These findings establish a quick and easy strategy for measuring visually-**
62 **evoked cortical activity with fNIRS that optimize the compliance of young**
63 **subjects, setting the background for testing the diagnostic value of fNIRS**
64 **visual measurements in the ASD clinical population.**

65

66

67

68

69

70

71

72

73 **Introduction**

74 Autism spectrum disorder (ASD) is a heterogeneous developmental condition that
75 involves persistent challenges in social interactions, restricted/repetitive behaviors,
76 and the lack of behavioral and cognitive flexibility¹. Since the pioneering work by
77 Lorna Wing², increasing epidemiological evidence indicates that autistic traits are
78 continuously distributed across the general population^{3,4}. This is due to the complex
79 genetic and epigenetic inheritance pattern of ASD, where multiple candidate loci
80 contribute to the pathogenesis of the disease^{5,6}. Milder autistic traits have been
81 termed the extended or broader autism phenotype (BAP), with BAP features being
82 particularly prevalent in first- and second-degree relatives of individuals with ASD⁶⁻⁹.
83 Since ASD and broader autistic manifestations share common genetic variants and
84 neurobiological susceptibility factors¹⁰, the general population emerges as a suitable
85 testing bed for the development of quantitative measures detecting neurostructural
86 and neurofunctional hallmarks of autism.

87 Over the last decade, the biological dimension of ASD has been largely
88 explored, thanks to the growing availability of advanced tools to explore brain
89 correlates of neurological disorders, including high-density EEG,
90 magnetoencephalography, positron emission tomography, magnetic resonance
91 imaging (MRI), and functional near-infrared spectroscopy (fNIRS)^{8,11,12}. A number of
92 studies reported defective neuroanatomical and neurofunctional features in
93 individuals with ASD, suggesting that a dysfunction of specific brain areas might
94 underlie the core symptoms of ASD¹³⁻¹⁷. Interestingly, similar neurological profiles
95 describe the relatives of autistic probands⁸.

96 fNIRS is an optical imaging technique that allows quantifying oxygen
97 consumption in different regions of the cerebral cortex, providing an indirect measure
98 of neuronal activity^{18,19}. This blood-oxygen-level-dependent (BOLD) signal is similar
99 to that detected with functional MRI (fMRI)²⁰. However, fNIRS is more tolerant to
100 motion artifacts than fMRI, and the development of robust methods for motion
101 detection and correction allowed to avoid sedation in children^{21,22}. Furthermore,
102 fNIRS has the advantage of being totally non-invasive, low-cost, portable, noiseless,
103 and endowed with high experimental flexibility and no setting constraints. This
104 methodological strength provides the fNIRS with a high ecological value for
105 investigating neural circuit maturation either in typically developing children or
106 clinically relevant populations^{21,23}.

107 Although the use of fNIRS in autism research is still an emerging area, a
108 number of studies aiming to decipher the neuronal mechanisms and circuits
109 underlying ASD evaluated different aspects of brain function and organization,
110 including resting-state and task-evoked responses^{24,25}. Coherence analyses of
111 resting-state hemodynamic activity showed weaker local and interhemispheric
112 functional connectivity in different cortical regions²⁶⁻³¹. Moreover, individuals on the
113 autism spectrum present patterns of atypical activity, including reduced
114 hemodynamic responses within specific brain regions, bilateral differences in
115 neuronal activation and the lack of cortical specialization, in tasks ranging from
116 sensory perception³² to executive functions³³, social perception³⁴⁻³⁷, joint attention³⁸⁻
117 ⁴⁰, imitation^{41,42}, facial and emotional processing⁴³⁻⁴⁶, speech perception and
118 language⁴⁷⁻⁵⁰. The majority of studies targeting evoked brain activity was focused on
119 the prefrontal and the temporal cortex²⁵, where symptom severity seems to be
120 inversely correlated with the degree of cortical activation^{42,43}.

121 Growing evidence suggests that fNIRS might be a candidate biomarker for
122 several neuropsychiatric disorders, including ASD^{29,51-55}. In particular, functional
123 network efficiency²⁹, weighted separability of NIRS signals⁵⁶, multi-layer neural
124 networks and sample entropy of spontaneous hemodynamic fluctuations^{54,57} have
125 been proposed as auxiliary diagnosis indexes for ASD. However, all these
126 approaches require complex algorithms to extract high-level features from the fNIRS
127 raw data, while fitness, applicability and translational value of biomarkers greatly
128 depend on their ease of use. In this framework, the analysis of visual phenotype has
129 become an important model to evaluate cortical processing in different
130 neurodevelopmental conditions⁵⁸⁻⁶³. Indeed, electrophysiological measurement of
131 visually evoked responses has been introduced as a quantitative method to assess
132 brain function in Rett syndrome^{58,64}, and hemodynamic responses (HDR) emerged
133 as a potential longitudinal biomarker for CDKL5 Deficiency Disorder and Creatine
134 Transporter Deficiency in murine models^{62,63}.

135 Since clinical studies suggested a dysregulation of sensory processing and
136 functional connectivity in the visual cortex of ASD subjects⁶⁵⁻⁶⁷, we hypothesized that
137 fNIRS visual measures could be related to broad autism dimensions in the general
138 population. To address this issue, we developed a novel standardized procedure to
139 assess HDR changes in the occipital cortex testing 40 randomly selected neuro-

140 typical adults and 19 children, and measuring inter-individual differences in autistic
141 traits, using the Autism-Spectrum Quotient (AQ^{68,69}).

142

143 **Results**

144 **An animated cartoon-based stimulus is able to evoke visual responses in the** 145 **adult cortex**

146 We measured the cortical HDR function⁷⁰ elicited by a reversing checkerboard
147 pattern in the adult population. In agreement with the previous literature^{71,72}, we
148 obtained a significant activation of the occipital cortex in response to different
149 conditions of visual stimulation (Fig. 1 and Fig. S1). Grand averages across adult
150 participants (see Table 1 for demographics) of Total Hb (THb), OxyHb (OHb) and
151 DeoxyHb (DHb) concentration changes are plotted in Fig. 2. Using a classic mean-
152 luminance grey screen as baseline, statistical analysis revealed a significant main
153 effect of the checkerboard stimulus (S) with respect to the blank presentation for all
154 HDR metrics (Radial Stimulus condition, RS, Fig. 2A).

155 To increase the entertaining quality of our experimental paradigm, we devised
156 an innovative visual stimulation protocol blending the checkerboard pattern with an
157 isoluminant commercial cartoon, thus serving as a reference baseline (Fig. 1 and
158 Fig. S1). We found a significant increase of THb and OHb, with a parallel reduction
159 of DHb concentration, in response to S appearance, reflecting the functional
160 activation of visual areas in this condition as well. The cortical response was
161 independent from the cartoon employed as baseline: a comparable HDR, indeed,
162 was clearly elicited both when the baseline movie was fixed a priori by the
163 experimenter (Cartoon Fixed condition, CF; Fig. 2B) and when the cartoon was
164 freely selected by the tested subject (Cartoon Chosen condition, CC; Fig. 2C).
165 Interestingly, a significant pattern of correlations emerged among HDR metrics
166 recorded with different stimulating conditions (Fig. S2), indicating that the quality of
167 visual input does not quantitatively impact HDR. The amplitude of cortical activation
168 was only slightly smaller in response to CF and CC, with the range of OHb and DHb
169 fluctuations being significantly lower with respect to that evoked by RS (Fig. 2D).

170 Within the CF condition, we also established that the baseline cartoon does
171 not affect the degree of visual activation: indeed, a comparable modification of THb,
172 OHb and DHb concentrations was recorded using “The Lion King”, “The Powerpuff
173 Girls”, “Peppa Pig” or “Kung Fu Panda” (Fig. S3A). Furthermore, no differences of

174 visually evoked responses were detected modulating the contrast level of the
175 baseline cartoon: THb, OHb and DHb fluctuations, indeed, were comparable when a
176 fixed baseline cartoon was presented at 20%, 40%, or 80% of contrast (Fig. 2E; Fig.
177 S3B-D). Finally, the response latency was homogenous in RS, CF, and CC
178 conditions (Fig. S4A).

179 Altogether, these results demonstrate the validity of this innovative stimulation
180 procedure to evoke a significant and reliable response in the occipital cortex
181 preserving inter-subject variability.

182

183 **The cartoon paradigm was reliable in eliciting cortical responses in children**

184 We measured cortical responses in typically developing children (see Table 2 for
185 demographics) viewing the radial checkerboard blended with the animated cartoon.
186 We compared three different conditions: each subject, indeed, was asked to select
187 two cartoons of their preference for the baseline and the first choice was employed
188 for the low-contrast (cartoon 1 low contrast, 20%, L1) and the high-contrast (cartoon
189 1 high contrast, 80%, H1) stimulation, while the second cartoon was presented only
190 at low-contrast (cartoon 2 low contrast, L2; Fig. S1).

191 Our data showed a significant activation of the visual cortex, with a prominent
192 change of THb, OHb and DHb concentration in response to the S with respect to the
193 blank for all conditions tested (Fig. 3A-C). The amplitude of elicited cortical
194 responses was comparable following L1, H1 and L2 (Fig. 3D), proving that the HDR
195 is independent from the cartoon narrative selected for the baseline and the contrast
196 level of baseline presentation in children as well. Small differences were observed
197 for response latency among L1, H1 and L2 conditions (Fig. S4B). A highly significant
198 pattern of correlations among different HDR indexes recorded in the diverse
199 conditions was detected (Fig. S5).

200 In agreement with previous literature⁷², a maturational trend of cortical
201 responsivity was recognized, with children showing significantly higher HDR
202 amplitude with respect to adult subjects (Fig. 3E). On the contrary, age-dependent
203 effects were not identified for response latency (Fig. S4C).

204 These findings establish a novel method for measuring visually-evoked
205 cortical activity with fNIRS that ensures an elevated compliance of young subjects
206 and high-quality reliability of measurements, suggesting a valuable tool for studying

207 visual cortical processing in typically developing children, but also in clinically
208 relevant populations.

209

210 **Negative correlation of HDR amplitude with AQ score**

211 Despite no effects detectable in adults (Fig. 4A-C), the amplitude of visual responses
212 was highly correlated to AQ scores in children (Fig. 4D-E). Consistent with a recent
213 work⁵⁴, the correlation was specific for THb, with higher AQ score being associated
214 with a lower amplitude of THb visually-evoked signals (Fig. 4D-E).

215 Interestingly, HDR amplitude was especially linked to social and
216 communication autistic traits (Fig. 5, S6): indeed, assessing separately the five AQ
217 subscales⁶⁹ we found a significant correlation of THb and OHb with the Social Skills
218 subscale (AQ_S, Fig. 5A-B), while only THb modulation was related to the
219 Communication subscale (AQ_C, Fig. 5C-D). Given the reliability across different
220 visual tasks (L1 and H1), the strongest interaction was between THb and AQ_S (Fig.
221 5A-B).

222

223 **Discussion**

224 We measured hemodynamic responses in the occipital cortex while subjects viewed
225 a reversing checkerboard pattern on a grey isoluminant baseline or the same
226 stimulus blended with a commercial animated cartoon. In all participants, the
227 patterned stimulus elicited a significant change of cortical Hb (upwards for THb and
228 OHb, down for DHb) independently from the reference baseline, while no response
229 was detected following blank presentation. Since HDR consists of an initial increase
230 in oxygen rich blood followed by a smaller depletion of deoxy-haemoglobin, with a
231 tight interrelation among total, oxygenated and reduced Hb levels, reporting all data
232 allows for a more accurate physiological interpretation of the results⁷⁰.

233 Interestingly, the level of occipital cortex activation did not depend on either
234 the movie selected as reference baseline or the baseline contrast, with only a slight
235 reduction of OHb and DHb change in response to the stimulus blended to animated
236 cartoons with respect to the classic RS condition. These data demonstrate the
237 reliability of this novel procedure with high entertaining and ecological value in
238 eliciting cortical activity. Thus, our approach might be helpful for studying cortical
239 function in children with an atypical trajectory of brain development, commonly
240 showing a reduced compliance in experimental environments.

241 The magnitude of HDR modulation, and in particular of THb, was inversely
242 correlated with AQ scores in children. Indeed, we found that the higher were the AQ
243 scores of subjects the lower was the amplitude of THb response to visual
244 stimulation, suggesting that visually-evoked fNIRS responses are able to capture the
245 dimension of autistic traits in the general young population. Our findings are
246 consistent with previous studies showing that cortical activation measured with
247 fNIRS and the performance in visual psychophysics negatively reflected ASD
248 symptom severity^{42,43,73–76}. Moreover, these data reinforce the concept that THb
249 changes could provide richer discriminative information for classifying between
250 typically developing children and ASD subjects⁵⁴. A tentative explanation of reduced
251 HDR in children with stronger autistic traits might be found in the difference of
252 perceptual styles in the general population^{77,78}: the preference for focusing on local
253 details vs. the global stimulus configuration, indeed, is a defining feature of ASD⁷⁹
254 and locally centered perception could be less effective in activating neural circuits of
255 visual cortex. Interestingly, a recent study established a vascular link to ASD,
256 showing early dysfunction of endothelial cells and impaired endothelium-dependent
257 vasodilation in a mouse model of 16p11.2 deletion⁸⁰. Since the HDR measured with
258 fNIRS strongly relies on neurovascular coupling, this suggests that lower
259 neurophysiological activity may stem in part from endothelial-dependent vascular
260 factors. In contrast, we failed to detect any correlation between HDR and AQ scores
261 in adult subjects. This is likely due to the different dynamic range and amplitude of
262 HDR responses measured in children and adult participants. Accordingly, the
263 maturation of neural and vascular networks over the first years of life affects
264 neurovascular coupling with a pattern of hemodynamic responses significantly
265 different in developing and adult brain⁸¹.

266 In our experiment, the THb index describes about 45% of the variance in AQ
267 scores. This correlation is remarkably high, considering that it is detected across two
268 separate visual stimulating procedures, i.e., the vision of low- and the high-contrast
269 blended RS-animated cartoons. Although the autistic questionnaire for children is
270 well-validated, showing good test-retest reliability and high internal consistency, not
271 all items have the same validity and factor analysis identified five subscales, named
272 ‘Social Skills’, ‘Communication’, ‘Attention to Detail’, ‘Imagination’ and ‘Attention
273 Switching’⁶⁹. We observed variability in the strength of correlation between HDR and
274 AQ subscales, with the highest correlation for the ‘Social Skills’ and ‘Communication’

275 subscales. Interestingly, ‘Social Skills’ and ‘Communication’ are the subscales with
276 higher construct validity performance in differentiating individuals with or without
277 ASD^{82,83}, while ‘Attention to Detail’ was the poorest classifying domain⁸⁴. It is also
278 worth stressing that among the items composing the ‘Attention to Detail’ subscale,
279 only four actually relate to sensory perception (e.g. ‘My child usually notices details
280 that others do not’), the others being more focused on cognitive functions (e.g. ‘My
281 child is fascinated by numbers’). Accordingly, the first pilot report of the AQ
282 questionnaire showed lower internal consistency (measured by Cronbach’s alpha
283 coefficient) of ‘Attention to Detail’ items compared to other subscales⁶⁸.

284 Although primarily affecting social functioning, there is a growing body of
285 evidence showing that ASD is also associated with abnormalities in multiple sensory
286 domains, fluctuating between hyper- and hypo-sensitivity to sensory stimuli^{73,85}. In
287 addition to a higher incidence of refractive errors and strabismus⁸⁶, anomalies in
288 visual processing, visual attention and visual-motor integration have been described
289 in ASD population^{66,73,87}. Interestingly, sensory symptoms are correlated with the
290 severity of the disorder, at least in children⁸⁸. Moreover, commonly observed
291 alterations in social skills might have a visual component⁷³ and perception deficits
292 could impact with cascading effects on the maturation of cognitive and social
293 domains⁸⁷.

294 It has been recently suggested that an early assessment of pupil size
295 modulation and visual behavior might improve the diagnostic process of
296 ASD^{66,77,87,89}. Currently, ASD diagnosis and follow-up almost entirely rely on
297 phenotypic information collected via clinical measures and parental input that are
298 highly prone to subjective bias⁹⁰. Moreover, the late appearance of some behavioral
299 autistic traits often delays the diagnosis until mid-childhood^{91,92}. Thus, the
300 identification of solid brain biomarkers early predicting ASD pathophysiology is a
301 critical step to anticipate tailored interventions, leading to better outcomes for
302 patients and possibly even the prevention of certain behaviors typically associated
303 with ASD. Objective biomarkers have also the potential to be helpful in the
304 management of patients, allowing the classification of disease severity and
305 monitoring response to treatments¹². A recent systematic review highlighted that
306 both functional and structural neuroimaging features might predict ASD diagnosis in
307 the early pre-symptomatic period^{93,94}, but further studies are needed to validate the
308 promising performance of such biomarkers¹². Lately, resting-state fNIRS

309 measurements have been suggested as candidate biomarkers for ASD^{29,54,56,57}. As
310 stressed above, fNIRS offers significant advantages with respect to other
311 neuroimaging tools, including non-invasiveness, ease of use, no need of sedation,
312 tolerance to movements and portability, making it a child-friendly approach.
313 However, the extraction of metrics with diagnostic value from resting-state
314 recordings involves complex algorithms.

315 In contrast, our analysis of visually evoked responses is quick, easy and
316 requires only that children pay attention to a short movie of their choice. Since our
317 stimulating strategy has been studied to optimize the compliance of young subjects,
318 we believe that our results might set the background for testing the predictive value
319 of fNIRS visual measurements to empower early detection of autistic traits.
320 Moreover, screening for autistic traits in the general population may be helpful in
321 epidemiological research because it may provide a large sample size to investigate
322 the correlation between autism phenotype severity and other pathophysiological
323 processes⁸³.

324

325 **Materials and methods**

326 **Subjects**

327 We recruited a total of 40 adult subjects (20 women, age: 31.05 ± 3.94 (SD) years)
328 and 19 children (5 girls, age: 7.20 ± 3.01 (SD) years). All participants reported
329 normal or corrected-to-normal vision and had no diagnosed neuropsychiatric
330 condition. Experimental procedures on children were authorized by the Regional
331 Pediatrics Ethics Board (Comitato Etico Pediatrico Regionale-Azienda Ospedaliero-
332 Universitaria Meyer-Firenze, Italy; authorization number 201/2019) and were
333 performed according to the declaration of Helsinki. Written informed consent was
334 obtained from all adult participants and from the parents of each child, authorizing
335 the use of anonymized data for research purposes. Assent was also obtained from
336 the children involved in the study before participation.

337

338 **AQ score**

339 Adult participants filled in the Autistic-traits Quotient (AQ) questionnaire, a 50-items
340 self-administered report validated for the Italian version^{68,95}. The items consist of
341 descriptive statements assessing personal preferences and typical behavior. For
342 each item, participants respond on a 4-point Likert scale: “strongly agree”, “slightly

343 agree”, “slightly disagree”, and “strongly disagree”. The items are grouped in five
344 subscales: Social Skills, Communication, Attention to Details, Imagination and
345 Attention Switching. All the questionnaires were scored by a neuropsychiatrist
346 blinded to subject data: 1 point was assigned when the participant’s response was
347 characteristic of ASD (slightly or strongly), 0 points were attributed otherwise. Total
348 scores range between 0 and 50, with 32 being the clinical threshold for autism risk⁶⁸.
349 No subjects scoring above 32 points were recorded. The mean (min-max) of the
350 scores was 15.0 (3-32) with SD of 6.5. Since child self-report might be affected by
351 reading and comprehension difficulties, the children's version of Autism Spectrum
352 Quotient (Italian version of AQ-child) was completed by parents⁶⁹. This version of the
353 AQ questionnaire includes 50 items as well, grouped in the same subscales
354 described above, and parents were required to report for each statement the degree
355 of consistency with their child’s behavior. Scores range from 0 to 150, since the
356 response scale is treated as a 4-point Likert scale with 0 representing definitely
357 agree; 1 slightly agree; 2 slightly disagree; and 3 definitely disagree. Items were
358 reverse scored as needed. The threshold score is 76⁶⁹. All subjects scored below 76
359 points. The mean (min-max) of the scores was 32.1 (17-49) with SD of 10.7.

360

361 **Apparatus and montages**

362 To measure changes in total Hb (THb) concentration and relative oxygenation levels
363 (OHb and DHb) in the occipital cortex during the task, we used a continuous-wave
364 NIRS system (NIRSport 8x8, NIRx Medical Technologies LLC, Berlin, Germany).
365 Our NIRSport system consists of 8 red light-sources operating at 760 nm and 850
366 nm, and 7 detectors which can be placed into a textile EEG cap (EASYCAP,
367 Herrsching, Germany), forming an array of 22 multi-distant channels⁹⁶. Textile EEG
368 caps of different sizes were used. The probe arrangement was fixed in each of the
369 caps using grommets, optode stabilizers, colored labels and holders in order to
370 assure comparable probe mapping over all subjects. For data recording, the Aurora
371 Software 1.4.1.1 (NIRx Medical Technologies LLC) was employed. The sampling
372 rate was 10.2 Hz. Visual areas were identified according to the craniocerebral
373 topography within the international 10-20 system and the placement of the optodes
374 was done using fOLD v2.2⁹⁷ and NIRSite 2.0 (NIRx Medical Technologies LLC)
375 softwares. Sources and detectors were symmetrically distributed to define 22
376 channels around the region of interest, each adjacent pair of sources and detectors

377 defining one channel (min-max source-detector separation: 20-44 mm for adults, 22-
378 30 mm for children; Fig. S2).

379

380 **Experimental Design and Visual Stimulation**

381 Prior to the experiment, adult participants (or parents for children) filled in the AQ
382 questionnaire. Then, subjects were asked to sit on a comfortable chair and the fNIRS
383 cap was positioned. Optodes were placed into the cap and the calibration of light
384 coupling between sensors and detectors was performed. All experimental sessions
385 lasted 30 minutes. Visual stimuli were generated using Python 3 and Psychopy3⁹⁸
386 and displayed with gamma correction on a monitor (Sharp LC-32LE352EWH, 60Hz
387 refresh rate, 45 cd/m² mean luminance, resolution of 800×600 pixels) placed 70 cm
388 from the subject. Cortical hemodynamics in response to full-field, reversing, square
389 wave, radial checkerboard, with abrupt phase inversion (spatial frequency: 0.33
390 cycles per degree, temporal frequency: 4 Hz; Fig. 1A) was evaluated in the time
391 domain by measuring the peak-to-baseline amplitude and latency. To have an
392 internal control with blank stimulation, we used an event-related design consisting of:
393 i) 20 cycles of 5 seconds stimulus 'on' (reversing checkerboard, 90% of contrast)
394 followed by 10 seconds stimulus 'off' and ii) 20 cycles of 5 seconds mock stimulus
395 'on' (reversing checkerboard, 0% of contrast) followed by 10 seconds stimulus 'off'.
396 The two stimulating conditions were pseudo randomly interleaved for each subject
397 during the recording. Blocks lasted 10 minutes and participants were permitted to
398 take rest between recordings. Fig. 1D shows a schematic representation of the
399 experimental procedure. Visual events were synchronized with NIRSport over
400 wireless LAN communication through the Python version of LabStreamingLayer
401 (<https://github.com/sccn/labstreaminglayer>).

402 Recordings in adult participants- Experiment 1 for adults (exp1) aimed to understand
403 whether a reliable hemodynamic signal could be recorded in response to the radial
404 checkerboard merged with an animated cartoon. Thus, exp1 started with a 10-
405 minutes recording using the reversing checkerboard as stimulus 'on' and the grey
406 screen as stimulus 'off' (RS condition), and continued with the vision of two different
407 blended animated cartoons, where the stimulus 'on' was a merge between the
408 reversing checkerboard and the movie, whereas the stimulus 'off' was the grey-scale
409 isoluminant cartoon (CF and CC conditions; Fig. S1). The merging procedure was
410 achieved using Python3 OpenCV⁹⁹. During the appearance of the stimulus each

411 frame was filtered using an automatic Canny edge detection algorithm
412 ([https://www.pyimagesearch.com/2015/04/06/zero-parameter-automatic-canny-](https://www.pyimagesearch.com/2015/04/06/zero-parameter-automatic-canny-edge-detection-with-python-and-opencv/)
413 [edge-detection-with-python-and-opencv/](https://www.pyimagesearch.com/2015/04/06/zero-parameter-automatic-canny-edge-detection-with-python-and-opencv/)), then the filtered cartoon was blended with
414 the radial checkerboard. Each pixel of the animated cartoon with the same color of
415 the corresponding pixel of the radial checkerboard was inverted, to obtain a fully
416 visible image. The result was a RS with an overlaid cartoon frame (Fig 1B). The
417 first cartoon was randomly selected by the operator within a group of 4 (“The Lion
418 King”, “The Powerpuff Girls”, “Peppa Pig” or “Kung Fu Panda”; CF), whereas the
419 latter was a free choice of the subject (CC). Exp2, aiming to dissect the contribution
420 of baseline contrast to visual responses, was performed in a subset of adult
421 participants (n = 15). Exp2 consisted of 3 consecutive recordings of a CF (“Peppa
422 Pig”; “Hide-and-see”, “Fly the kite”, “Polly parrot” episodes) with the modulation of
423 the baseline contrast (20%, 40%, 80%; Fig. S1). The presentation order of different
424 contrast levels was randomly shuffled.

425 Recordings in children- To confirm that the baseline movie and its contrast do not
426 affect the emergence of visual responses to the radial checkerboard in children, we
427 measured hemodynamic signals in response to 2 different blended RS-animated
428 cartoons freely decided by the subject: cartoon 1 was presented at both low (20%,
429 L1) and high (80%, H1) contrast, while only low contrast was recorded for cartoon 2
430 (L2; Fig. S1). In this case, the presentation order was decided by the child, in order
431 to maximize subject compliance.

432 During the experimental sessions, data were quickly analyzed and visualized using
433 nirsLAB software (NIRx Medical Technologies LLC, v2019.4).

434

435 **Signal Processing and Statistical analysis**

436 Data preprocessing was completed using the Homer3 package (v1.29.8) in MATLAB
437 (R2020a). We created a processing stream tailored on recent guidelines for analysis
438 of fNIRS data²². First, the raw intensity data were converted to optical density (OD)
439 changes (*hmR_Intensity2OD*). Then, channels showing very high or low optical
440 intensity were excluded from further analyses using the function
441 *hmR_PruneChannels* (dRange: 5e-04-1e+00, SNRthresh: 2; SDrange: 0.0-45.0).
442 Motion artifacts were then removed by a multistep rejection protocol. After a step of
443 motion artifact detection using the *hmR_MotionArtifactByChannel* function (tMotion:
444 1.0, tMask: 1.0; STDEVthresh 13.0; AMPthresh: 0.40), motion correction was

445 performed with a combination of Spline interpolation (*hmR_MotionCorrectSpline*, p:
446 0.99) and Wavelet filtering (*hmR_MotionCorrectWavelet*, iqr: 0.80) functions²². The
447 remaining uncorrected motion artifacts were identified using the
448 *hmR_MotionArtifactByChannel*. A band-pass filter (*hmR_BandpassFilt*:
449 *Bandpass_Filter_OpticalDensity*, hpf: 0.01, lpf: 0.50) was applied to decrease slow
450 drifts and high-frequency noise, and the OD data were converted to Hb
451 concentration changes using the modified Beer–Lambert law (*hmR_OD2Conc*, ppf:
452 1.0 1.0 1.0). Finally, trials of each subject were block-averaged for every stimulating
453 condition and channel (*hmR_BlockAvg: Block_Average_on_Concentration_Data*,
454 trange: -2.0 20.0)²². The resulting txt file was imported in Python as a Pandas
455 DataFrame. For each subject, only the channel with the highest response amplitude
456 was analyzed. The peak response was identified as the maximal value for THb and
457 OHb and the minimum value for DHb. A grand average was taken of the 20 trials of
458 data per stimulating condition and differences between visual stimulation ‘on’
459 (reversing checkerboard) and ‘off’ (blank) were compared. All data were normalised
460 with respect to the blank-evoked response using a subtraction method. Statistical
461 analysis was carried out using *pingouin* Python library¹⁰⁰ and the following functions:
462 *pingouin.ttest* (paired and two-sided t-test), *pingouin.rm_anova* (one-way repeated
463 measures ANOVA), *pingouin.pairwise_ttests* (post-hoc analysis),
464 *pingouin.pairwise_corr* (Spearman correlation), *pingouin.regplot* (Linear regression).
465 T-test, ANOVA and post-hoc analysis were used to assess differences in fNIRS peak
466 responses following different stimulating conditions, whereas we tested the
467 interaction between the amplitude of fNIRS measures and AQ scores with Spearman
468 correlation and we employed the Linear regression to plot such correlation.
469 Adjustments for multiple comparisons were performed using the Benjamini/Hochberg
470 false discovery rate (BH-FDR) correction. The effect size calculated for the ANOVA
471 was the generalized eta-squared. All the plots have been generated using *Matplotlib*
472 Python library¹⁰¹. All statistical metrics and details are reported in Table S1.

473

474 **Data availability**

475 The datasets generated during the current study and scripts used for visual
476 stimulation are available, respectively on Zenodo
477 (<http://doi.org/10.5281/zenodo.5101912>) and GitHub website
478 (https://github.com/raffaelemazziotti/FNIRS_code).

479

480 **References**

- 481 1. Maenner, M. J. *et al.* Potential impact of DSM-5 criteria on autism spectrum
482 disorder prevalence estimates. *JAMA Psychiatry* **71**, 292–300 (2014).
- 483 2. Wing, L. The Continuum of Autistic Characteristics. *Diagnosis and Assessment*
484 *in Autism* 91–110 (1988) doi:10.1007/978-1-4899-0792-9_7.
- 485 3. Posserud, M.-B., Lundervold, A. J. & Gillberg, C. Autistic features in a total
486 population of 7-9-year-old children assessed by the ASSQ (Autism Spectrum
487 Screening Questionnaire). *J. Child Psychol. Psychiatry* **47**, 167–175 (2006).
- 488 4. Ruzich, E. *et al.* Measuring autistic traits in the general population: a systematic
489 review of the Autism-Spectrum Quotient (AQ) in a nonclinical population sample
490 of 6,900 typical adult males and females. *Mol. Autism* **6**, 2 (2015).
- 491 5. Persico, A. M. & Bourgeron, T. Searching for ways out of the autism maze:
492 genetic, epigenetic and environmental clues. *Trends Neurosci.* **29**, 349–358
493 (2006).
- 494 6. Ruzich, E. *et al.* Subgrouping siblings of people with autism: Identifying the
495 broader autism phenotype. *Autism Res.* **9**, 658–665 (2016).
- 496 7. Piven, J., Palmer, P., Jacobi, D., Childress, D. & Arndt, S. Broader autism
497 phenotype: evidence from a family history study of multiple-incidence autism
498 families. *Am. J. Psychiatry* **154**, 185–190 (1997).
- 499 8. Billeci, L. *et al.* The Broad Autism (Endo)Phenotype: Neurostructural and
500 Neurofunctional Correlates in Parents of Individuals with Autism Spectrum
501 Disorders. *Front. Neurosci.* **10**, 346 (2016).
- 502 9. Carpita, B. *et al.* The broad autism phenotype in real-life: clinical and functional
503 correlates of autism spectrum symptoms and rumination among parents of
504 patients with autism spectrum disorder. *CNS Spectr.* **25**, 765–773 (2020).
- 505 10. Bralten, J. *et al.* Autism spectrum disorders and autistic traits share genetics and
506 biology. *Mol. Psychiatry* **23**, 1205–1212 (2018).
- 507 11. Pagnozzi, A. M., Conti, E., Calderoni, S., Fripp, J. & Rose, S. E. A systematic
508 review of structural MRI biomarkers in autism spectrum disorder: A machine
509 learning perspective. *Int. J. Dev. Neurosci.* **71**, 68–82 (2018).
- 510 12. Frye, R. E. *et al.* Emerging biomarkers in autism spectrum disorder: a systematic
511 review. *Ann Transl Med* **7**, 792 (2019).

- 512 13. Amaral, D. G., Schumann, C. M. & Nordahl, C. W. Neuroanatomy of autism.
513 *Trends Neurosci.* **31**, 137–145 (2008).
- 514 14. Bellani, M., Calderoni, S., Muratori, F. & Brambilla, P. Brain anatomy of autism
515 spectrum disorders I. Focus on corpus callosum. *Epidemiol. Psychiatr. Sci.* **22**,
516 217–221 (2013).
- 517 15. Bellani, M., Calderoni, S., Muratori, F. & Brambilla, P. Brain anatomy of autism
518 spectrum disorders II. Focus on amygdala. *Epidemiol. Psychiatr. Sci.* **22**, 309–
519 312 (2013).
- 520 16. Billeci, L. *et al.* On the application of quantitative EEG for characterizing autistic
521 brain: a systematic review. *Front. Hum. Neurosci.* **7**, 442 (2013).
- 522 17. Calderoni, S., Bellani, M., Hardan, A. Y., Muratori, F. & Brambilla, P. Basal
523 ganglia and restricted and repetitive behaviours in Autism Spectrum Disorders:
524 current status and future perspectives. *Epidemiol. Psychiatr. Sci.* **23**, 235–238
525 (2014).
- 526 18. Lloyd-Fox, S., Blasi, A. & Elwell, C. E. Illuminating the developing brain: the past,
527 present and future of functional near infrared spectroscopy. *Neurosci. Biobehav.*
528 *Rev.* **34**, 269–284 (2010).
- 529 19. Gervain, J. *et al.* Near-infrared spectroscopy: a report from the McDonnell infant
530 methodology consortium. *Dev. Cogn. Neurosci.* **1**, 22–46 (2011).
- 531 20. Raichle, M. E. & Mintun, M. A. Brain work and brain imaging. *Annu. Rev.*
532 *Neurosci.* **29**, 449–476 (2006).
- 533 21. Vanderwert, R. E. & Nelson, C. A. The use of near-infrared spectroscopy in the
534 study of typical and atypical development. *Neuroimage* **85 Pt 1**, 264–271 (2014).
- 535 22. Di Lorenzo, R. *et al.* Recommendations for motion correction of infant fNIRS
536 data applicable to multiple data sets and acquisition systems. *Neuroimage* **200**,
537 511–527 (2019).
- 538 23. Yamasaki, T. *et al.* Rapid maturation of voice and linguistic processing systems
539 in preschool children: a near-infrared spectroscopic study. *Exp. Neurol.* **250**,
540 313–320 (2013).
- 541 24. Mazzoni, A., Grove, R., Eapen, V., Lenroot, R. K. & Bruggemann, J. The
542 promise of functional near-infrared spectroscopy in autism research: What do we
543 know and where do we go? *Soc. Neurosci.* **14**, 505–518 (2019).
- 544 25. Zhang, F. & Roeyers, H. Exploring brain functions in autism spectrum disorder:
545 A systematic review on functional near-infrared spectroscopy (fNIRS) studies.

- 546 *Int. J. Psychophysiol.* **137**, 41–53 (2019).
- 547 26. Keehn, B., Wagner, J. B., Tager-Flusberg, H. & Nelson, C. A. Functional
548 connectivity in the first year of life in infants at-risk for autism: a preliminary near-
549 infrared spectroscopy study. *Front. Hum. Neurosci.* **7**, 444 (2013).
- 550 27. Zhu, H., Fan, Y., Guo, H., Huang, D. & He, S. Reduced interhemispheric
551 functional connectivity of children with autism spectrum disorder: evidence from
552 functional near infrared spectroscopy studies. *Biomed. Opt. Express* **5**, 1262–
553 1274 (2014).
- 554 28. Li, J. *et al.* Characterization of autism spectrum disorder with spontaneous
555 hemodynamic activity. *Biomed. Opt. Express* **7**, 3871–3881 (2016).
- 556 29. Li, Y. & Yu, D. Weak network efficiency in young children with Autism Spectrum
557 Disorder: Evidence from a functional near-infrared spectroscopy study. *Brain*
558 *and Cognition* vol. 108 47–55 (2016).
- 559 30. Jia, H., Li, Y. & Yu, D. Attenuation of long-range temporal correlations of
560 neuronal oscillations in young children with autism spectrum disorder.
561 *Neuroimage Clin* **20**, 424–432 (2018).
- 562 31. Cao, W. *et al.* The Development of Brain Network in Males with Autism
563 Spectrum Disorders from Childhood to Adolescence: Evidence from fNIRS
564 Study. *Brain Sci* **11**, (2021).
- 565 32. Xu, M., Minagawa, Y., Kumazaki, H., Okada, K.-I. & Naoi, N. Prefrontal
566 Responses to Odors in Individuals With Autism Spectrum Disorders: Functional
567 NIRS Measurement Combined With a Fragrance Pulse Ejection System. *Front.*
568 *Hum. Neurosci.* **14**, 523456 (2020).
- 569 33. Xiao, T. *et al.* Response inhibition impairment in high functioning autism and
570 attention deficit hyperactivity disorder: evidence from near-infrared spectroscopy
571 data. *PLoS One* **7**, e46569 (2012).
- 572 34. Lloyd-Fox, S. *et al.* Reduced neural sensitivity to social stimuli in infants at risk
573 for autism. *Proc. Biol. Sci.* **280**, 20123026 (2013).
- 574 35. Braukmann, R. *et al.* Diminished socially selective neural processing in 5-month-
575 old infants at high familial risk of autism. *Eur. J. Neurosci.* **47**, 720–728 (2018).
- 576 36. Lloyd-Fox, S. *et al.* Cortical responses before 6 months of life associate with
577 later autism. *Eur. J. Neurosci.* **47**, 736–749 (2018).
- 578 37. Bhat, A. N., McDonald, N. M., Eilbott, J. E. & Pelphrey, K. A. Exploring cortical
579 activation and connectivity in infants with and without familial risk for autism

- 580 during naturalistic social interactions: A preliminary study. *Infant Behav. Dev.* **57**,
581 101337 (2019).
- 582 38. Iwanaga, R. *et al.* Usefulness of near-infrared spectroscopy to detect brain
583 dysfunction in children with autism spectrum disorder when inferring the mental
584 state of others. *Psychiatry Clin. Neurosci.* **67**, 203–209 (2013).
- 585 39. Zhu, B. & Godavarty, A. Functional connectivity in the brain in joint attention
586 skills using near infrared spectroscopy and imaging. *Behav. Brain Res.* **250**, 28–
587 31 (2013).
- 588 40. Zhu, H. *et al.* Atypical prefrontal cortical responses to joint/non-joint attention in
589 children with autism spectrum disorder (ASD): A functional near-infrared
590 spectroscopy study. *Biomed. Opt. Express* **6**, 690–701 (2015).
- 591 41. Tamura, R., Kitamura, H., Endo, T., Abe, R. & Someya, T. Decreased leftward
592 bias of prefrontal activity in autism spectrum disorder revealed by functional
593 near-infrared spectroscopy. *Psychiatry Res.* **203**, 237–240 (2012).
- 594 42. Su, W.-C. *et al.* Differences in cortical activation patterns during action
595 observation, action execution, and interpersonal synchrony between children
596 with or without autism spectrum disorder (ASD): An fNIRS pilot study. *PLoS One*
597 **15**, e0240301 (2020).
- 598 43. Kita, Y. *et al.* Self-face recognition in children with autism spectrum disorders: a
599 near-infrared spectroscopy study. *Brain Dev.* **33**, 494–503 (2011).
- 600 44. Nakadoi, Y. *et al.* Multi-channel near-infrared spectroscopy shows reduced
601 activation in the prefrontal cortex during facial expression processing in
602 pervasive developmental disorder. *Psychiatry Clin. Neurosci.* **66**, 26–33 (2012).
- 603 45. Fox, S. E., Wagner, J. B., Shrock, C. L., Tager-Flusberg, H. & Nelson, C. A.
604 Neural processing of facial identity and emotion in infants at high-risk for autism
605 spectrum disorders. *Front. Hum. Neurosci.* **7**, 89 (2013).
- 606 46. Mori, K. *et al.* Neuroimaging in autism spectrum disorders: 1H-MRS and NIRS
607 study. *J. Med. Invest.* **62**, 29–36 (2015).
- 608 47. Minagawa-Kawai, Y. *et al.* Cerebral laterality for phonemic and prosodic cue
609 decoding in children with autism. *Neuroreport* **20**, 1219–1224 (2009).
- 610 48. Funabiki, Y., Murai, T. & Toichi, M. Cortical activation during attention to sound
611 in autism spectrum disorders. *Res. Dev. Disabil.* **33**, 518–524 (2012).
- 612 49. Edwards, L. A., Wagner, J. B., Tager-Flusberg, H. & Nelson, C. A. Differences in
613 Neural Correlates of Speech Perception in 3 Month Olds at High and Low Risk

- 614 for Autism Spectrum Disorder. *J. Autism Dev. Disord.* **47**, 3125–3138 (2017).
- 615 50. Pecukonis, M., Perdue, K. L., Wong, J., Tager-Flusberg, H. & Nelson, C. A.
616 Exploring the relation between brain response to speech at 6-months and
617 language outcomes at 24-months in infants at high and low risk for autism
618 spectrum disorder: A preliminary functional near-infrared spectroscopy study.
619 *Dev. Cogn. Neurosci.* **47**, 100897 (2021).
- 620 51. Yasumura, A. *et al.* Age-related differences in frontal lobe function in children
621 with ADHD. *Brain Dev.* **41**, 577–586 (2019).
- 622 52. Chou, P.-H., Huang, C.-J. & Sun, C.-W. The Potential Role of Functional Near-
623 Infrared Spectroscopy as Clinical Biomarkers in Schizophrenia. *Curr. Pharm.*
624 *Des.* **26**, 201–217 (2020).
- 625 53. Husain, S. F. *et al.* Validating a functional near-infrared spectroscopy diagnostic
626 paradigm for Major Depressive Disorder. *Sci. Rep.* **10**, 9740 (2020).
- 627 54. Xu, L. *et al.* Characterizing autism spectrum disorder by deep learning
628 spontaneous brain activity from functional near-infrared spectroscopy. *J.*
629 *Neurosci. Methods* **331**, 108538 (2020).
- 630 55. Yang, D., Hong, K.-S., Yoo, S.-H. & Kim, C.-S. Evaluation of Neural
631 Degeneration Biomarkers in the Prefrontal Cortex for Early Identification of
632 Patients With Mild Cognitive Impairment: An fNIRS Study. *Front. Hum. Neurosci.*
633 **13**, 317 (2019).
- 634 56. Yanagisawa, K., Nakamura, N., Tsunashima, H. & Narita, N. Proposal of
635 auxiliary diagnosis index for autism spectrum disorder using near-infrared
636 spectroscopy. *Neurophotonics* **3**, 031413 (2016).
- 637 57. Xu, L. *et al.* Identification of autism spectrum disorder based on short-term
638 spontaneous hemodynamic fluctuations using deep learning in a multi-layer
639 neural network. *Clin. Neurophysiol.* **132**, 457–468 (2021).
- 640 58. Durand, S. *et al.* NMDA receptor regulation prevents regression of visual cortical
641 function in the absence of *Mecp2*. *Neuron* **76**, 1078–1090 (2012).
- 642 59. de Freitas Dotto, P. *et al.* Sweep visually evoked potentials and visual findings in
643 children with West syndrome. *Eur. J. Paediatr. Neurol.* **18**, 201–210 (2014).
- 644 60. Begenisic, T., Sansevero, G., Baroncelli, L., Cioni, G. & Sale, A. Early
645 environmental therapy rescues brain development in a mouse model of Down
646 syndrome. *Neurobiol. Dis.* **82**, 409–419 (2015).
- 647 61. Boggio, E. M. *et al.* Visual impairment in FOXP1-mutated individuals and mice.

- 648 *Neuroscience* **324**, 496–508 (2016).
- 649 62. Mazziotti, R. *et al.* Searching for biomarkers of CDKL5 disorder: early-onset
650 visual impairment in CDKL5 mutant mice. *Hum. Mol. Genet.* **26**, 2290–2298
651 (2017).
- 652 63. Mazziotti, R. *et al.* Novel translational phenotypes and biomarkers for creatine
653 transporter deficiency. *Brain Commun* **2**, fcaa089 (2020).
- 654 64. LeBlanc, J. J. *et al.* Visual evoked potentials detect cortical processing deficits in
655 Rett syndrome. *Ann. Neurol.* **78**, 775–786 (2015).
- 656 65. Keehn, B., Westerfield, M. & Townsend, J. Brief Report: Cross-Modal Capture:
657 Preliminary Evidence of Inefficient Filtering in Children with Autism Spectrum
658 Disorder. *J. Autism Dev. Disord.* **49**, 385–390 (2019).
- 659 66. Little, J.-A. Vision in children with autism spectrum disorder: a critical review.
660 *Clin. Exp. Optom.* **101**, 504–513 (2018).
- 661 67. Seymour, R. A., Rippon, G., Gooding-Williams, G., Schoffelen, J. M. & Kessler,
662 K. Dysregulated oscillatory connectivity in the visual system in autism spectrum
663 disorder. *Brain* **142**, 3294–3305 (2019).
- 664 68. Baron-Cohen, S., Wheelwright, S., Skinner, R., Martin, J. & Clubley, E. The
665 autism-spectrum quotient (AQ): evidence from Asperger syndrome/high-
666 functioning autism, males and females, scientists and mathematicians. *J. Autism*
667 *Dev. Disord.* **31**, 5–17 (2001).
- 668 69. Auyeung, B., Baron-Cohen, S., Wheelwright, S. & Allison, C. The Autism
669 Spectrum Quotient: Children's Version (AQ-Child). *J. Autism Dev. Disord.* **38**,
670 1230–1240 (2008).
- 671 70. Tachtsidis, I. & Scholkmann, F. False positives and false negatives in functional
672 near-infrared spectroscopy: issues, challenges, and the way forward.
673 *Neurophotonics* **3**, 031405 (2016).
- 674 71. Chen, L.-C., Sandmann, P., Thorne, J. D., Herrmann, C. S. & Debener, S.
675 Association of Concurrent fNIRS and EEG Signatures in Response to Auditory
676 and Visual Stimuli. *Brain Topogr.* **28**, 710–725 (2015).
- 677 72. Ward, L. M., Aitchison, R. T., Tawse, M., Simmers, A. J. & Shahani, U. Reduced
678 Haemodynamic Response in the Ageing Visual Cortex Measured by Absolute
679 fNIRS. *PLoS One* **10**, e0125012 (2015).
- 680 73. Simmons, D. R. *et al.* Vision in autism spectrum disorders. *Vision Res.* **49**,
681 2705–2739 (2009).

- 682 74. Park, W. J., Schauder, K. B., Zhang, R., Bennetto, L. & Tadin, D. High internal
683 noise and poor external noise filtering characterize perception in autism
684 spectrum disorder. *Sci. Rep.* **7**, 17584 (2017).
- 685 75. Noel, J.-P., Lakshminarasimhan, K. J., Park, H. & Angelaki, D. E. Increased
686 variability but intact integration during visual navigation in Autism Spectrum
687 Disorder. *Proc. Natl. Acad. Sci. U. S. A.* **117**, 11158–11166 (2020).
- 688 76. Noel, J.-P., Zhang, L.-Q., Stocker, A. A. & Angelaki, D. E. Individuals with autism
689 spectrum disorder have altered visual encoding capacity. *PLoS Biol.* **19**,
690 e3001215 (2021).
- 691 77. Turi, M., Burr, D. C. & Binda, P. Pupillometry reveals perceptual differences that
692 are tightly linked to autistic traits in typical adults. *Elife* **7**, (2018).
- 693 78. Tortelli, C., Turi, M., Burr, D. C. & Binda, P. Objective pupillometry shows that
694 perceptual styles covary with autistic-like personality traits. *Elife* **10**, (2021).
- 695 79. Hallen, R. V. der *et al.* Global processing takes time: A meta-analysis on local–
696 global visual processing in ASD. *Psychological Bulletin* vol. 141 549–573 (2015).
- 697 80. Ouellette, J. *et al.* Vascular contributions to 16p11.2 deletion autism syndrome
698 modeled in mice. *Nat. Neurosci.* **23**, 1090–1101 (2020).
- 699 81. Kozberg, M. & Hillman, E. Neurovascular coupling and energy metabolism in the
700 developing brain. *Prog. Brain Res.* **225**, 213–242 (2016).
- 701 82. Broadbent, J., Galic, I. & Stokes, M. A. Validation of Autism Spectrum Quotient
702 Adult Version in an Australian Sample. *Autism Research and Treatment* vol.
703 2013 1–7 (2013).
- 704 83. Lundqvist, L.-O. & Lindner, H. Is the Autism-Spectrum Quotient a Valid Measure
705 of Traits Associated with the Autism Spectrum? A Rasch Validation in Adults
706 with and Without Autism Spectrum Disorders. *J. Autism Dev. Disord.* **47**, 2080–
707 2091 (2017).
- 708 84. Wouters, S. G. M. & Spek, A. A. The use of the Autism-spectrum Quotient in
709 differentiating high-functioning adults with autism, adults with schizophrenia and
710 a neurotypical adult control group. *Research in Autism Spectrum Disorders* vol.
711 5 1169–1175 (2011).
- 712 85. Leekam, S. R., Nieto, C., Libby, S. J., Wing, L. & Gould, J. Describing the
713 sensory abnormalities of children and adults with autism. *J. Autism Dev. Disord.*
714 **37**, 894–910 (2007).
- 715 86. Scharre, J. E. & Creedon, M. P. Assessment of visual function in autistic

- 716 children. *Optom. Vis. Sci.* **69**, 433–439 (1992).
- 717 87. Apicella, F., Costanzo, V. & Purpura, G. Are early visual behavior impairments
718 involved in the onset of autism spectrum disorders? Insights for early diagnosis
719 and intervention. *European Journal of Pediatrics* vol. 179 225–234 (2020).
- 720 88. Kern, J. K. *et al.* Sensory correlations in autism. *Autism* vol. 11 123–134 (2007).
- 721 89. Jones, W. & Klin, A. Attention to eyes is present but in decline in 2-6-month-old
722 infants later diagnosed with autism. *Nature* **504**, 427–431 (2013).
- 723 90. McPartland, J. C. *et al.* Looking Back at the Next 40 Years of ASD Neuroscience
724 Research. *J. Autism Dev. Disord.* (2021) doi:10.1007/s10803-021-05095-5.
- 725 91. Baird, G., Cass, H. & Slonims, V. Diagnosis of autism. *BMJ* **327**, 488–493
726 (2003).
- 727 92. Zwaigenbaum, L. *et al.* Stability of diagnostic assessment for autism spectrum
728 disorder between 18 and 36 months in a high-risk cohort. *Autism Res.* **9**, 790–
729 800 (2016).
- 730 93. Emerson, R. W. *et al.* Functional neuroimaging of high-risk 6-month-old infants
731 predicts a diagnosis of autism at 24 months of age. *Sci. Transl. Med.* **9**, (2017).
- 732 94. Hazlett, H. C. *et al.* Early brain development in infants at high risk for autism
733 spectrum disorder. *Nature* **542**, 348–351 (2017).
- 734 95. Ruta, L., Mazzone, D., Mazzone, L., Wheelwright, S. & Baron-Cohen, S. The
735 Autism-Spectrum Quotient--Italian version: a cross-cultural confirmation of the
736 broader autism phenotype. *J. Autism Dev. Disord.* **42**, 625–633 (2012).
- 737 96. Vrana, A., Meier, M. L., Hotz-Boendermaker, S., Humphreys, B. K. &
738 Scholkman, F. Cortical Sensorimotor Processing of Painful Pressure in Patients
739 with Chronic Lower Back Pain-An Optical Neuroimaging Study using fNIRS.
740 *Front. Hum. Neurosci.* **10**, 578 (2016).
- 741 97. Zimeo Morais, G. A., Balardin, J. B. & Sato, J. R. fNIRS Optodes' Location
742 Decider (fOLD): a toolbox for probe arrangement guided by brain regions-of-
743 interest. *Sci. Rep.* **8**, 3341 (2018).
- 744 98. Peirce, J. *et al.* PsychoPy2: Experiments in behavior made easy. *Behav. Res.*
745 *Methods* **51**, 195–203 (2019).
- 746 99. Gollapudi, S. OpenCV with Python. *Learn Computer Vision Using OpenCV* 31–
747 50 (2019) doi:10.1007/978-1-4842-4261-2_2.
- 748 100. Vallat, R. Pingouin: statistics in Python. *Journal of Open Source Software* vol.
749 3 1026 (2018).

750 101. Hunter, J. D. Matplotlib: A 2D Graphics Environment. *Computing in Science &*
751 *Engineering* vol. 9 90–95 (2007).

752

753

754 **Acknowledgements:** This work was supported by a Telethon grant from GP19177
755 to LB, and a grant from University of Pisa (PRA-2020-50) to RB.

756

757 **Author contribution:** RB, GC and LB conceived the study. RM, ES, EC, VM, RR
758 and LB designed the experiments. RM, ES and LB carried out the research. RM, ES
759 and LB analyzed the data. LB wrote the manuscript. All authors were involved in the
760 revision of the draft manuscript and have agreed to the final content.

761

762 **Conflict of Interest:** The authors declare no competing financial interests.

763

764

765 **Figure legends**

766 **Fig.1: Visual stimulation and experimental paradigm. A:** Representative frame of
767 baseline grey screen (upper row, stimulus ‘off’) and reversing checkerboard (lower
768 row, stimulus ‘on’) for RS condition. The small black square indicates the fixation
769 point. **B:** Representative frame of low-contrast (20%) grey-scale baseline animated
770 cartoon (upper row, stimulus ‘off’) and blended checkerboard-cartoon (lower row,
771 stimulus ‘on’) for CF and CC conditions. **C:** Representative HDR in the occipital
772 cortex during the stimulus ‘off’ (upper row) and stimulus ‘on’ activation phase (lower
773 row) according to the output of nirsLAB software. The Look Up table is reported
774 under the images. **D:** Experimental protocol showing that the cycles of visual
775 stimulation were structured in blocks of 40 trials (20 trials with the reversing
776 checkerboard and 20 trials with the ‘mock’ stimulus) for a total duration of 10
777 minutes.

778

779 **Fig. 2: HDR was reliably detected in adults using both RS and blended RS-**
780 **animated cartoons.** For all panels, values in the y-axis are multiplied for 10^4 . **A:**
781 On the left, the average time course for THb (green line), OHb (red line) and DHb
782 (blue line) in response to the RS are shown. The three plots on the right depict the

783 average peak response to the stimulus (S) vs. the blank (B) across all the adult
784 subjects. The stimulus-driven signal was significantly different from the blank for all
785 the conditions (t-test, $p < 0.001$ for all comparisons). **B:** Same plots as above for the
786 CF condition. On the left, the average time course of the evoked HDR is depicted.
787 On the right, the graphs showed that the HDR amplitude was significantly higher in
788 response to S with respect to B for THb, OHb and DHb (t-test, $p < 0.001$ for all
789 comparisons). **C:** CC condition. Also in this case the S elicited significantly higher
790 responses for THb, OHb and DHb with respect to the B (t-test, $p < 0.001$ for all
791 comparisons). **D:** Comparison among different visual stimulations (RS: Radial
792 Stimulus, CF: fixed cartoon, CC: chosen cartoon) shows no differences in evoked
793 amplitudes for THb, whereas a significant difference was detected between RS and
794 CC for OHb (One-way RM ANOVA, $p < 0.01$, post hoc BH-FDR, RS vs. CC $p < 0.01$)
795 and a more complex pattern of differences emerged for DHb (One-way RM ANOVA,
796 $p < 0.001$, post hoc BH-FDR, RS vs. CF $p < 0.01$, RS vs. CC $p < 0.001$, CF vs CC p
797 < 0.05). **E:** No differences of evoked responses were detected with different contrast
798 levels of the baseline movie (L: low, M: medium, H: high). For statistical metrics and
799 details, refer to table S1. Data are shown as average \pm s.e.m. * $p < 0.05$; ** $p < 0.01$;
800 *** $p < 0.001$.

801

802 **Fig. 3: HDR signal was reliably detected in children using blended RS-animated**
803 **cartoons with low and high contrast.** For all panels, values in the y-axis are
804 multiplied for 10^4 . **A:** On the left, the average time course for THb (green line), OHb
805 (red line) and DHb (blue line) in response to low-contrast (20%) blended RS-
806 animated cartoons is shown. On the right, the graphs represent the average
807 amplitude of the evoked HDR following the stimulus (S) and the blank (B). A
808 significantly different response to S with respect to the B was detectable for all
809 metrics (t-test, $p < 0.001$ for all comparisons). **B:** The average time course of the
810 HDR to high-contrast (80%) blended RS-animated cartoons is shown. Here, the
811 baseline cartoon is the same as the experiment described in panel A, but a different
812 part of the movie was used. THb, OHb and DHb showed a significantly higher
813 deflection to the S with respect to the B in this condition as well (t-test, $p < 0.001$ for
814 all comparisons). **C:** On the left, the average time course of HDR following the
815 second low-contrast blended RS-animated cartoon selected by the subject. On the
816 right, the analysis of peak amplitudes revealed significantly higher responses during

817 S compared to B for THb, OHb and DHb (t-test, $p < 0.001$ for all comparisons). **D:**
818 Comparison among different contrast levels of the baseline cartoon revealed no
819 differences in the amplitude of HDR. **E:** Response amplitudes for low-contrast
820 blended RS-animated cartoons in adults and children. More specifically, we
821 compared the response to CF condition of adults with L1 condition for children. The
822 average amplitude of HDR was significantly higher in children (t-test, $p < 0.001$ for
823 THb, $p < 0.05$ for OHb, $p < 0.01$ for DHb). For statistical metrics and details, refer to
824 table S1. Data are shown as average \pm s.e.m. * $p < 0.05$; ** $p < 0.01$; *** $p < 0.001$.

825

826 **Fig. 4: Correlation between HDR and AQ scores.** For all panels, values in the x-
827 axis are multiplied for 10^4 . The ρ (rho) index in each plot indicates the Spearman
828 correlation value. **A-C:** Correlation between HDR and AQ scores in adults, for
829 amplitudes obtained using RS (**A**), CF (**B**), and CC (**C**). No significant correlations
830 were detected for adult participants. **D-E:** Correlation between HDR and AQ scores
831 in children, for amplitudes obtained using high (**D**), and low (**E**) contrast baseline
832 cartoons. A significant correlation was found between THb and AQ scores for both
833 high- and low-contrast blended stimuli ($p < 0.05$ for both cases). Circles are
834 individual values, lines represent the linear regression model fit and shaded regions
835 are the 95% CI.

836

837 **Fig. 5: Correlation between HDR and AQ subscales in children.** For all panels,
838 values in the x-axis are multiplied for $\times 10^4$. The ρ (rho) index in each plot indicates
839 the Spearman correlation value. **A-B:** Correlations between HDR and AQ Social
840 Skills (AQ_S) subscale. A significant correlation between THb and AQ_S was
841 detected using both high- (A) and low-contrast blended stimuli (B; $p < 0.05$ for both
842 cases). In addition, OHb recorded in response to the low-contrast blended RS-
843 cartoon was significantly correlated with AQ_S (B; $p < 0.05$). **C-D:** Correlations
844 between HDR and AQ Communication (AQ_C) subscale. THb amplitude in response
845 to the high-contrast blended RS-cartoon was significantly correlated with AQ_C ($p <$
846 0.05). Circles are individual values, lines represent the linear regression model fit
847 and shaded regions are the 95% CI.

848

849 **Table 1:** Demographic characteristics of adult subjects. Age (years), gender, head
850 circumference (head, cm), cap size (cm), total AQ score (AQ), AQ subscale scores

851 (AQ_S, AQ_C, AQ_A, AQ_D, AQ_I) and the movies used for visual stimulation (CF
852 and CC according to the experimental protocol) are listed for each participant. For
853 movies, production company, release date and episode title are indicated as well.

854

855 **Table 2:** Demographic characteristics of children. Age (years), gender, head
856 circumference (head, cm), cap size (cm), total AQ score (AQ), AQ subscale scores
857 (AQ_S, AQ_C, AQ_A, AQ_D, AQ_I) and the movies used for visual stimulation (C1
858 and C2 according to the experimental protocol) are listed for each participant. For
859 movies, production company, release date and episode title are indicated as well.

860

Fig 1

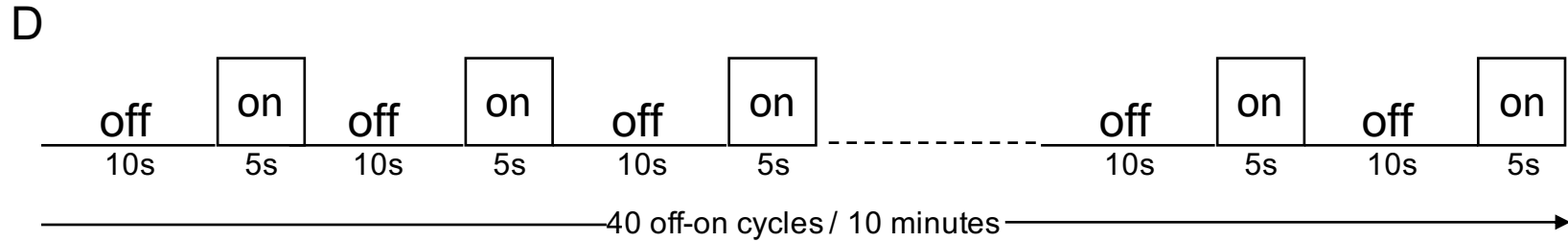
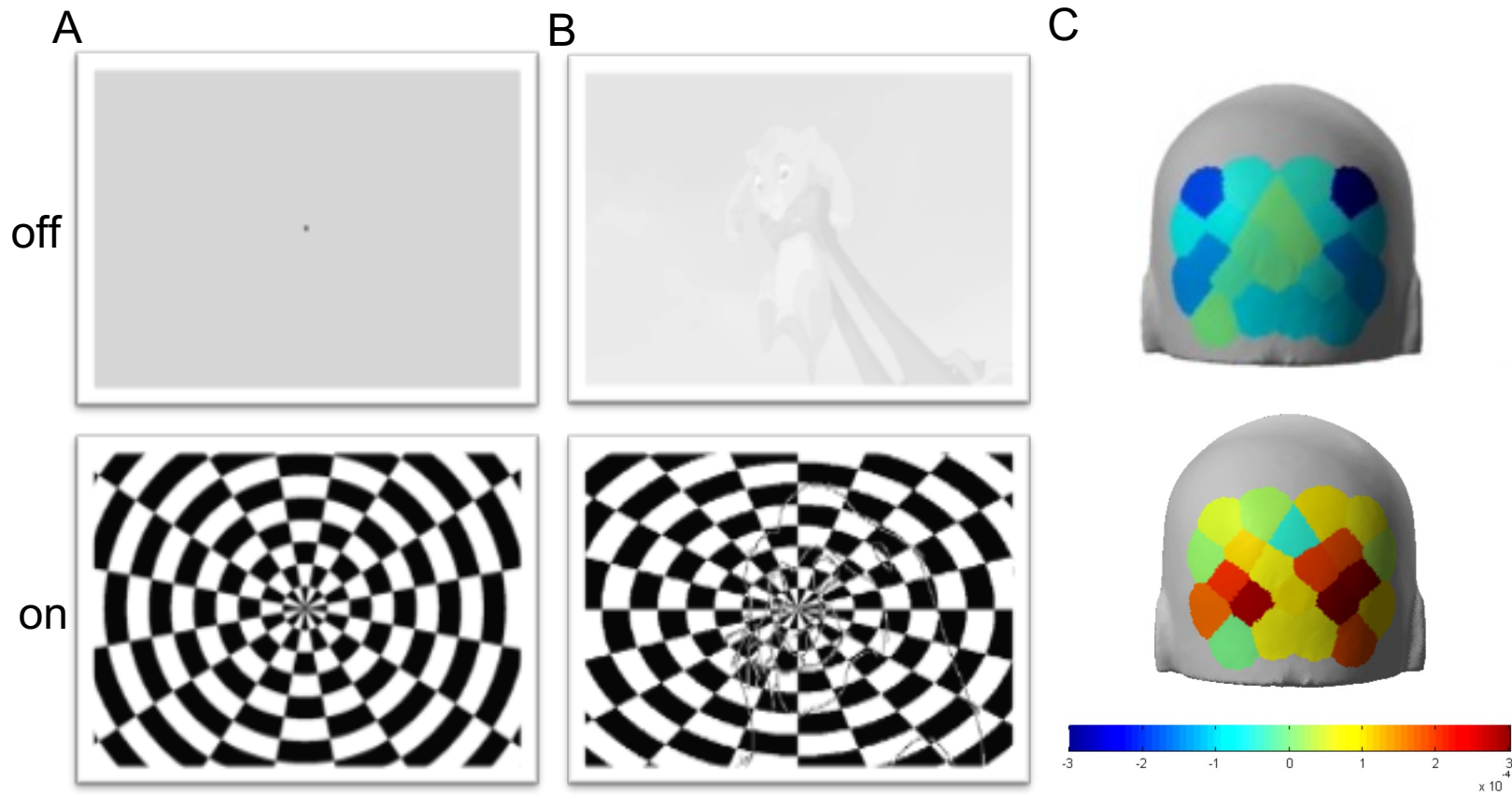


Fig 2

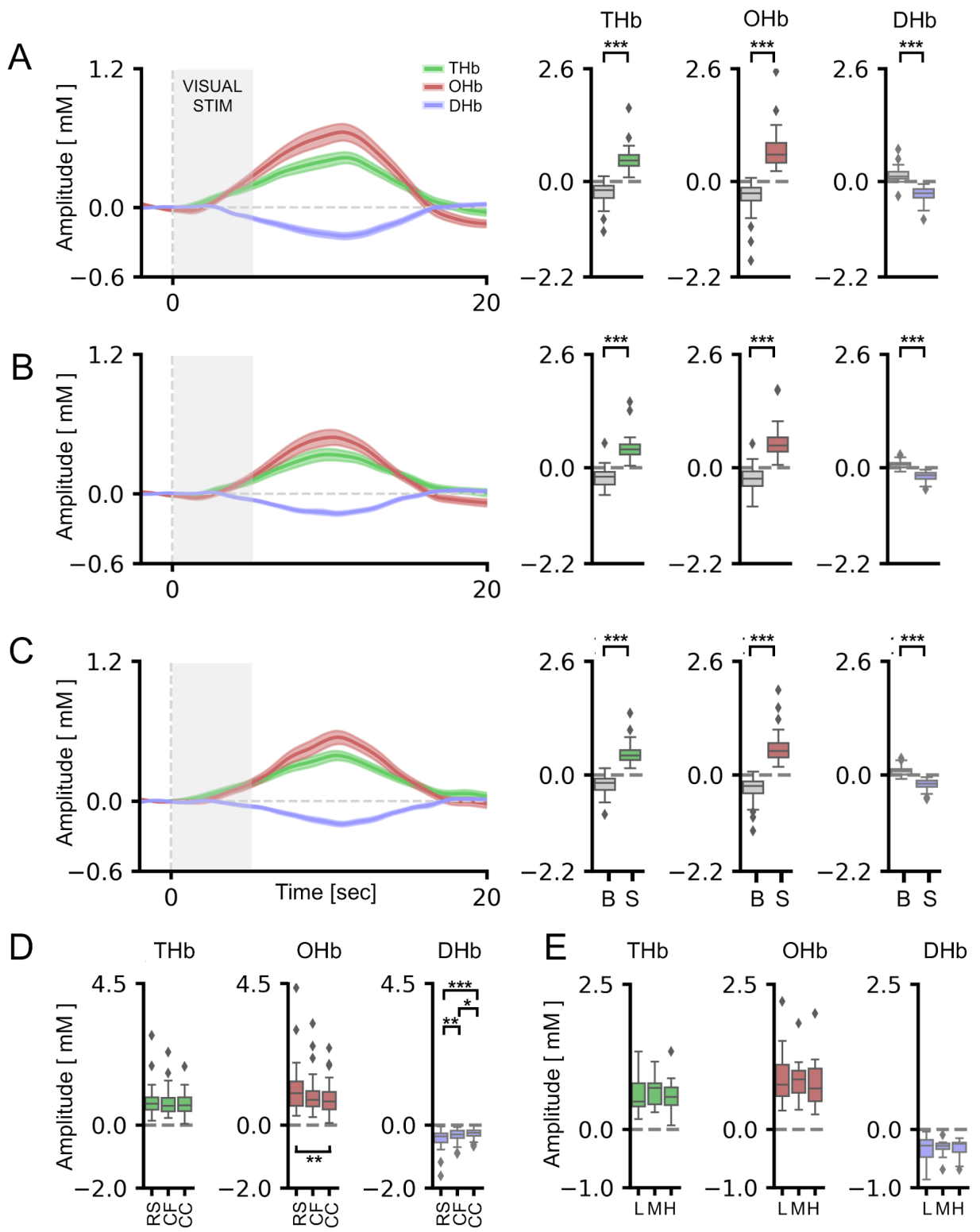


Fig 3

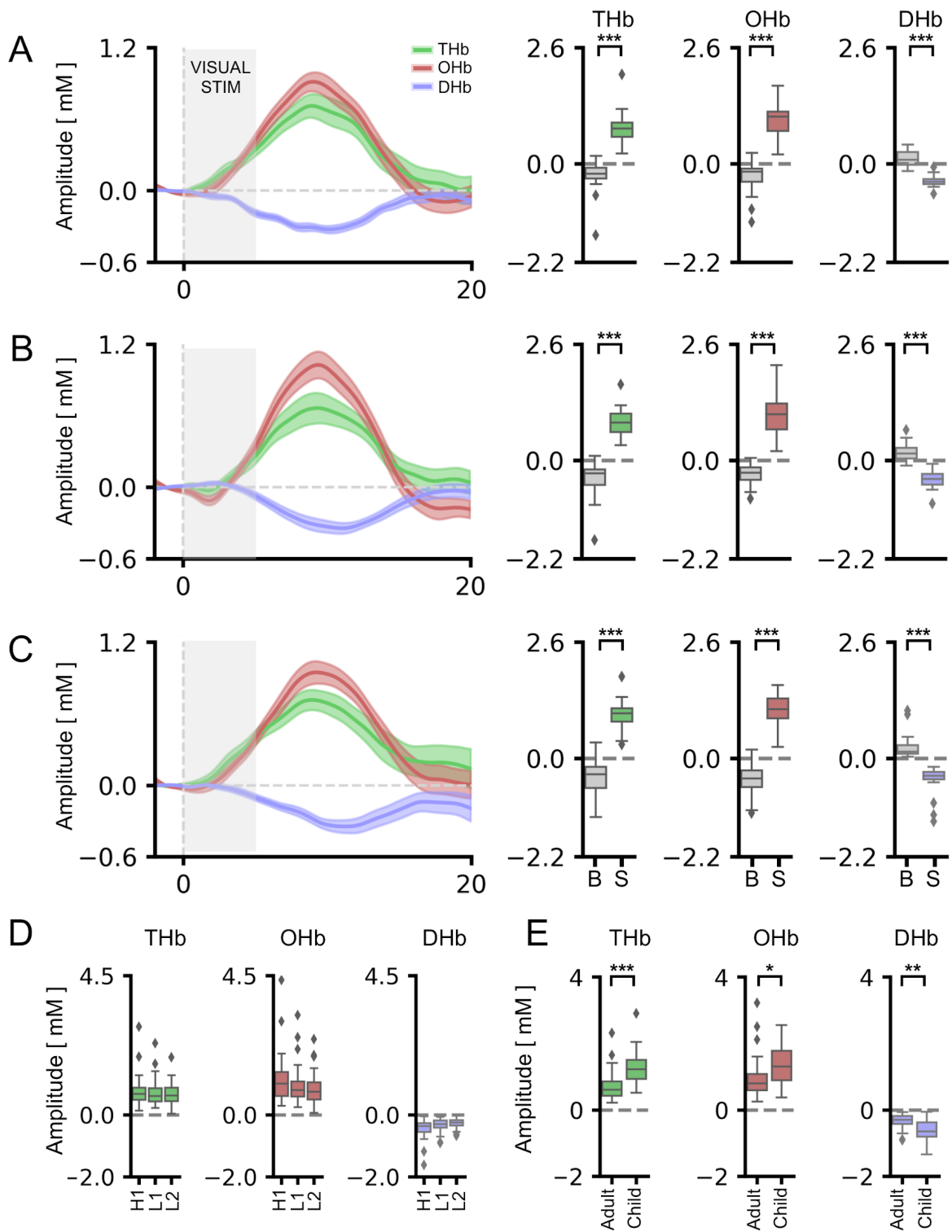


Fig 4

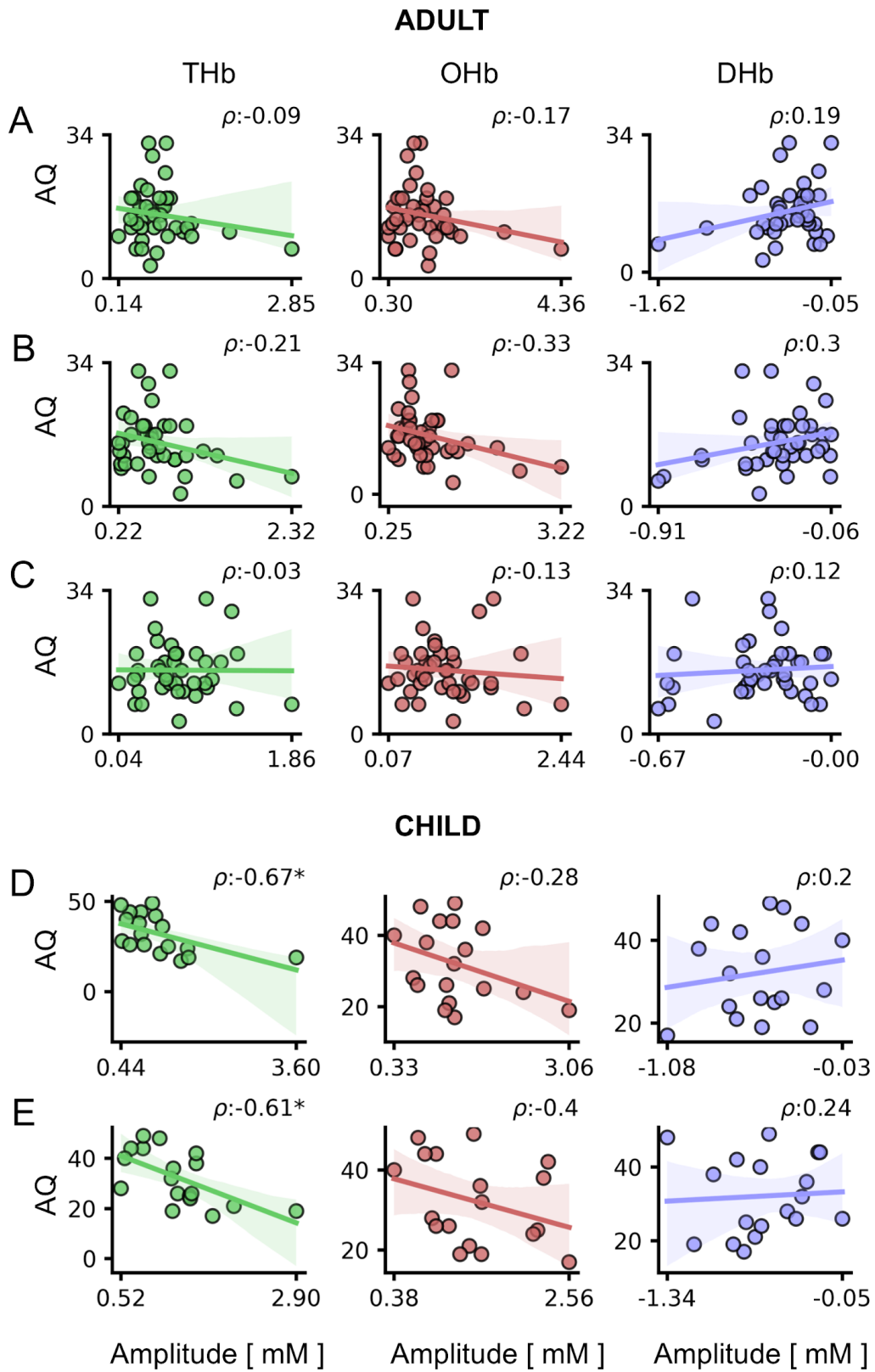
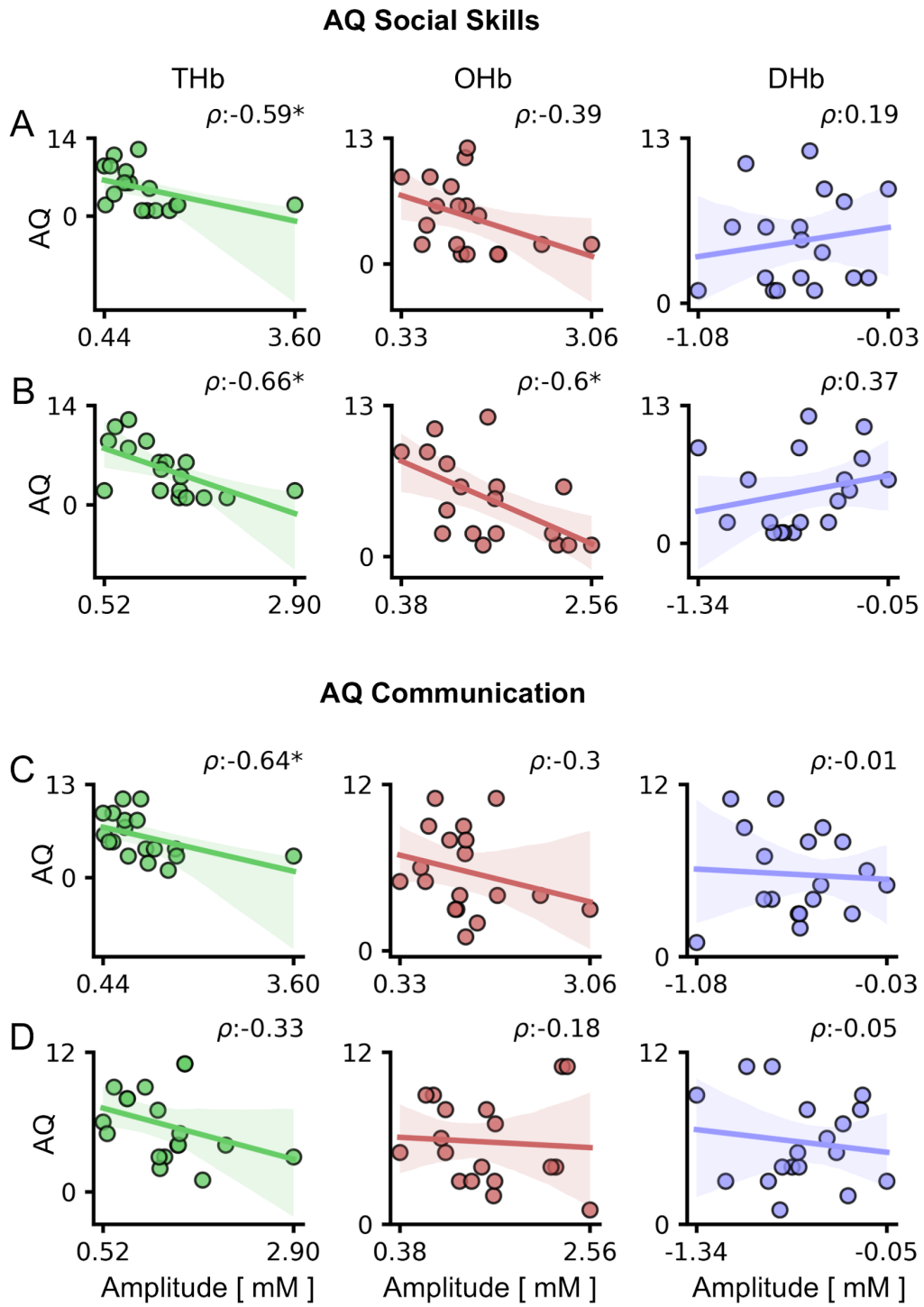


Fig 5



ID	Age	Gender	Head	Cap size	AQ	AQ_S	AQ_C	AQ_A	AQ_D	AQ_I	CF	CC
A1	29	F	57	56	11	0	1	7	1	2	The Lion King Walt Disney Pictures,1994	The Sword in the Stone Walt Disney Productions,1963
A2	36	F	56	56	17	0	0	6	9	2	The Powerpuff Girls special episode "Twas the Fight Before Christmas", Cartoon Network Studios, 2003	The Aristocats Walt Disney Productions,1970
A3	35	M	57	56	17	3	3	5	0	6	Kung Fu Panda DreamWorks Animation, 2008	Aladdin Walt Disney Pictures,1992
A4	28	F	57	56	3	0	0	1	1	1	Peppa Pig "Hide-and-seek", "Fly the kite", "Polly parrot" episodes, Entertainment One, 2004	The Simpsons S29E02 "Springfield Splendor", 20th Television, 2017
A5	25	F	57	56	19	4	1	7	6	1	The Lion King Walt Disney Pictures,1994	101 Dalmatians Walt Disney Productions,1961
A6	35	F	57	56	15	4	2	4	5	0	The Powerpuff Girls special episode "Twas the Fight Before Christmas", Cartoon Network Studios, 2003	The Simpsons S29E02 "Springfield Splendor", 20th Television, 2017
A7	29	F	57	56	11	0	2	5	3	1	Peppa Pig "Hide-and-seek", "Fly the kite", "Polly parrot" episodes, Entertainment One, 2004	101 Dalmatians Walt Disney Productions,1961
A8	30	F	56	56	13	0	2	4	5	2	Kung Fu Panda DreamWorks Animation, 2008	Wall-E Disney-Pixar, 2008
A9	29	F	59	56	7	1	1	3	2	0	The Lion King Walt Disney Pictures,1994	The Sword in the Stone Walt Disney Productions,1963
A10	29	M	58	56	12	1	1	5	4	1	The Powerpuff Girls special episode "Twas the Fight Before Christmas", Cartoon Network Studios, 2003	Aladdin Walt Disney Pictures,1992
A11	27	M	56.5	56	17	2	3	5	4	3	Peppa Pig "Hide-and-seek", "Fly the kite", "Polly parrot" episodes, Entertainment One, 2004	101 Dalmatians Walt Disney Productions,1961
A12	30	F	56	56	9	1	2	2	3	1	Kung Fu Panda DreamWorks Animation, 2008	Inside out Disney-Pixar, 2015
A13	29	M	57	56	14	1	3	6	2	2	The Lion King Walt Disney Pictures,1994	Wall-E Disney-Pixar, 2008
A14	36	M	58.5	56	19	2	2	5	7	3	The Powerpuff Girls special episode "Twas the Fight Before Christmas", Cartoon Network Studios, 2003	101 Dalmatians Walt Disney Productions,1961
A15	36	M	57	56	16	4	1	4	5	2	Peppa Pig "Hide-and-seek", "Fly the kite", "Polly parrot" episodes, Entertainment One, 2004	Aladdin Walt Disney Pictures,1992
A16	29	F	54	56	22	1	3	9	7	2	Kung Fu Panda DreamWorks Animation, 2008	The Rescuers Walt Disney Productions,1977
A17	28	F	58.5	56	7	1	0	2	1	3	The Lion King Walt Disney Pictures,1994	101 Dalmatians Walt Disney Productions,1961
A18	29	F	55	56	12	0	1	5	5	1	The Powerpuff Girls special episode "Twas the Fight Before Christmas", Cartoon Network Studios, 2003	Peter Pan Walt Disney Productions,1953
A19	34	M	60	56	19	6	2	5	5	1	Peppa Pig "Hide-and-seek", "Fly the kite", "Polly parrot" episodes, Entertainment One, 2004	SpongeBob S12E01 "FarmerBob", Nickelodeon Animation Studio, 2018
A20	26	M	58	56	10	3	0	5	2	0	Kung Fu Panda DreamWorks Animation, 2008	Inside out Disney-Pixar, 2015

A21	36	F	56	56	15	1	2	2	7	3	The Lion King Walt Disney Pictures,1994	Inside out Disney-Pixar, 2015
A22	30	M	60.5	56	19	1	2	6	4	6	The Lion King Walt Disney Pictures,1994	The Sword in the Stone Walt Disney Productions,1963
A23	26	F	56	56	12	0	1	5	6	0	The Powerpuff Girls special episode "Twas the Fight Before Christmas", Cartoon Network Studios, 2003	Wall-E Disney-Pixar, 2008
A24	32	M	60.5	56	7	0	1	5	0	1	Kung Fu Panda DreamWorks Animation, 2008	Aladdin Walt Disney Pictures,1992
A25	34	F	56	56	10	1	1	4	2	2	The Lion King Walt Disney Pictures1994	Beauty and the Beast Walt Disney Pictures,1994
A26	29	F	57	56	32	6	5	8	9	4	The Powerpuff Girls special episode "Twas the Fight Before Christmas", Cartoon Network Studios, 2003	The Aristocats Walt Disney Productions,1970
A27	31	M	59	56	32	10	6	6	2	8	Kung Fu Panda DreamWorks Animation, 2008	The Simpsons S29E02 "Springfield Splendor", 20th Television, 2017
A28	39	F	57	56	21	2	4	4	8	3	Peppa Pig "Hide-and-seek", "Fly the kite", "Polly parrot" episodes, Entertainment One, 2004	Lady Oscar, "A Funeral Bell Tolls in the Twilight" episode, Discotek Media, 1980
A29	29	M	57	56	6	0	0	2	2	2	The Lion King Walt Disney Pictures,1994	The Simpsons S29E02 "Springfield Splendor", 20th Television, 2017
A30	29	M	57	56	17	3	2	5	6	1	The Powerpuff Girls special episode "Twas the Fight Before Christmas", Cartoon Network Studios, 2003	The Sword in the Stone Walt Disney Productions,1963
A31	36	M	59.5	56	12	0	0	6	4	2	Peppa Pig "Hide-and-seek", "Fly the kite", "Polly parrot" episodes, Entertainment One, 2004	The Sword in the Stone Walt Disney Productions,1963
A32	27	M	59	56	12	1	2	5	2	2	The Powerpuff Girls special episode "Twas the Fight Before Christmas", Cartoon Network Studios, 2003	The Aristocats Walt Disney Productions,1970
A33	40	M	57	56	13	2	3	1	6	1	Peppa Pig "Hide-and-seek", "Fly the kite", "Polly parrot" episodes, Entertainment One, 2004	The Simpsons S29E02 "Springfield Splendor", 20th Television, 2017
A34	31	F	55	56	15	1	1	4	4	5	Kung Fu Panda DreamWorks Animation, 2008	The Sword in the Stone Walt Disney Productions,1963
A35	27	M	56.5	56	19	6	2	4	7	0	The Lion King Walt Disney Pictures,1994	Frozen Walt Disney Pictures, 2013
A36	30	M	58	56	14	5	1	3	4	1	The Powerpuff Girls special episode "Twas the Fight Before Christmas", Cartoon Network Studios, 2003	Wall-E Disney-Pixar, 2008
A37	25	M	58	56	29	6	8	6	7	2	Peppa Pig "Hide-and-seek", "Fly the kite", "Polly parrot" episodes, Entertainment One, 2004	Wall-E Disney-Pixar, 2008
A38	31	M	57.5	56	10	0	1	5	3	1	Kung Fu Panda DreamWorks Animation, 2008	Inside out Disney-Pixar, 2015
A39	38	M	57.5	56	25	2	4	6	8	5	The Lion King Walt Disney Pictures,1994	The Sword in the Stone Walt Disney Productions,1963
A40	33	F	57.5	56	13	0	0	3	10	0	The Powerpuff Girls special episode "Twas the Fight Before Christmas", Cartoon Network Studios, 2003	Beauty and the Beast Walt Disney Pictures,1994

ID	Age	Gender	Head	Cap size	AQ	AQ-S	AQ_C	AQ_A	AQ_D	AQ_I	C1 (L1 and H1)	C2 (L2)
B1	5	M	51.5	52	21	1	4	7	5	4	Uncle Grandpa S3E04 "Uncle Easter", Cartoon Network Studios, 2016	Teen Titans Go! To the Movies Warner Bros. Animation, 2018
B2	5	M	51	52	32	6	7	3	10	6	Wile E. Coyote & Road Runner "Coyote falls", ""Fur of flying" and "Rabid rider" episodes, Acme Corporation, 2010	ABCs song Little Baby Bum - Nursery Rhymes & Kids Songs youtube channel, 2014
B3	13	M	57	56	26	6	3	4	7	6	The Simpsons S29E02 "Springfield Splendor", 20th Television, 2017	Futurama, S7E01 "The Bots and the Bees", Comedy Central, 2012
B4	12	M	56	56	44	8	8	11	13	4	The Incredibles Disney-Pixar, 2004	Wile E. Coyote & Road Runner "Coyote falls", ""Fur of flying" and "Rabid rider" episodes, Acme Corporation, 2010
B5	12	M	56	56	25	1	4	10	0	10	Big Hero 6 Walt Disney Pictures, 2014	The Amazing World of Gumball S01E01 "The DVD", Cartoon Network Development Studio Europe, 2011
B6	6	F	53	52	17	1	1	4	8	3	Inside out Disney-Pixar, 2015	Floopaloo S1E22 "Squirrel for a Day", Marc du Pontavice, 2012
B7	7	M	53	52	24	2	4	1	12	5	The Chipmunks "Bye, George" episode, DIC Entertainment, 1989	Floopaloo S1E22 "Squirrel for a Day", Marc du Pontavice, 2012
B8	4	F	50.5	52	38	6	11	7	11	3	Frozen Walt Disney Pictures, 2013	Bolt Walt Disney Pictures, 2008
B9	4	M	52	52	42	1	11	11	13	6	Spider-Man: Into the Spider-Verse Columbia Pictures, 2018	Bolt Walt Disney Pictures, 2008
B10	4	M	51	52	n.a.	n.a.	n.a.	n.a.	n.a.	n.a.	Cars Walt Disney Pictures, 2006	Thomas & Friends "Diesel and the duckling" episode, Mattel, 2019
B11	9	F	54	56	28	2	6	3	13	4	The Simpsons S29E02 "Springfield Splendor", 20th Television, 2017	Zig & Sharko S01E28 "Moby Zig", Xilam Animation, 2010
B12	8	M	54.5	56	26	4	5	5	4	8	Beauty and the Beast Walt Disney Pictures,1994	Ice Age Blue Sky Studios, 2002
B13	4	M	53	56	44	11	9	8	9	7	Finding Nemo Disney-Pixar 2003	101 Dalmatians Walt Disney Productions,1961
B14	6	M	53	52	36	5	2	3	19	7	Trolls DreamWorks Animation, 2016	Curious George S1E03 "Zeros to Donuts", Universal Animation Studios, 2006
B15	7	M	51.5	52	49	12	8	10	9	10	Cars Walt Disney Pictures, 2006	Pup Academy S1E02 "Tell Us About Your Human Day", Air Bud Entertainment, 2019
B16	10	F	55	56	48	9	9	10	10	10	Frozen Walt Disney Pictures, 2013	Descendants Disney Channel Original Productions, 2015
B17	10	M	54	56	40	9	5	7	13	6	The Simpsons S29E02 "Springfield Splendor", 20th Television, 2017	Uncle Grandpa S3E04 "Uncle Easter", Cartoon Network Studios, 2016
B18	4	F	49.5	52	19	2	3	5	6	3	Frozen Walt Disney Pictures, 2013	Bing S1E06 "Smoothie", Tandem Films e Digitales Studios, 2014
B19	7	M	54	56	19	2	3	5	6	3	Ranger Rob S1E12 "Big Stink in Big Sky Park" Nelvana Enterprises Inc, 2016	Arex&Vastatore "Casket of fear" episode Arex&Vastatore YouTube Channel, 2021